Electronic Supplementary Information (ESI) for Chemical Communications This journal is (c) The Royal Society of Chemistry 2024

Gold brocade coated CoFe PBA with enhanced peroxidase-like activity for chemiluminescent imaging immunoassay

Ling Li,[a,‡] Qingwen Chen,[a,‡] Feng Shi,[a,‡] Jiayu Wu,[a] Lingfeng Min,[b,*] Juan Li,[a,*] Zhanjun Yang[a,*]

[a] *School of Chemistry and Chemical Engineering, Yangzhou University, Yangzhou 225002, P.R. China*

[b] *Clinical Medical College of Yangzhou University, Northern Jiangsu People's Hospital, Yangzhou 225001, P.R. China*

Experimental

Materials and Reagents. The HIgG, rabbit anti-HIgG and goat anti-HIgG was purchased from Bioss Antibodies Biotechnology Co., Ltd. (Beijing). Bovine serum albumin (BSA), chitosan, 1-(3-Dimethylaminopropyl)-3-ethylcarbodiimide hydrochloride (EDC), Pluronic F-127, N-Hydroxysuccinimide (NHS), 3-glycidoxypropyltrimethoxysilane (GPTMS, 98%) and 11-Mercaptoundecanoic acid (MUA) were purchased from Sigma-Aldrich. 3,3',5,5'-tetramethylbenzidine (TMB) and luminol were purchased from America Acros. Thermosetting insulating paint AC-3G is purchased from JUJO Chemical Co. (Japan). P-iodophenol (PIP) was purchased from Alfa Aesar (China). Trisodium citrate dihydrate ($C_6H_5Na_3O_7 \cdot 2H_2O$), tetrachloroauric acid trihydrate ($HAuCl_4 \cdot 3H_2O$), hydrogen peroxide (H_2O_2), disodium phosphate (Na_2HPO_4), potassium dihydrogen phosphate (KH_2PO_4), cobaltous nitrate hexahydrate ($Co(NO_3)_2 \cdot 6H_2O$), potassium ferricyanide ($K_3[Fe(CN)_6]$), sodium hydroxide (NaOH), sodium borohydride ($NaBH_4$), sodium chloride (NaCl), methylbenzene and potassium chloride (KCl) were supplied by Sinopharm Chemical Reagent Co., Ltd. (Shanghai). All the biological reagents prepared were dissolved or diluted using phosphate buffer solution (PBS) and stored in refrigerator at 4 ℃ before measurements.

The PBS was prepared by dissolving 1.37 mM NaCl, 2.7 mM KCl, 8.72 mM

Na_2HPO_4 and 1.42 mM KH_2PO_4 in deionized water and its pH is 7.4. The Piranha Acid was prepared from H_2SO_4 and 30 wt% H_2O_2 in the ratio of 7:3 by volume. Tris-HCl buffer solution was prepared by dissolving 1.25 g of Tris in 100 mL deionized water and the pH was adjusted to 8.5 with HCl. The luminol reserve solution (0.01 M) was prepared by dissolving 177 mg of luminol in NaOH solution (0.1 M). The PIP reserve solution (0.01 mol/L) was obtained by dissolving 110 mg PIP in 5 mL dimethyl sulfoxide and diluting it to 50 mL with deionized water. Before use, luminol and PIP reserve solution were pre-mixed and diluted with Tris-HCl buffer (0.1 M, pH 8.5). Chemiluminescence (CL) substrate includes 5 mM luminol, 0.6 mM PIP and 4 mM H_2O_2. All other reagents are of analytical grade and deionized water were used in the experiments.

Apparatus. CL measurements were carried out on a luminescence imaging system (Protein Simple Co., USA). All measurements were performed at (25 ± 1)°C under stagnant. CL array chips was fabricated on Electric Vertical Plane Screen Printing Machine (Foshan Shunde Lunjiao Jingyida Printing Machinery Factory). Scanning electron microscope (SEM) images were obtained by Hitachi S-4800 scanning electron microscope (Japan) at accelerated voltage 15 kV. Transmission electron micrographs (TEM) were obtained via utilizing a JEM-2100 Emission transmission electron microscope (Japan) at an acceleration voltage of 120 kV. Ultraviolet-visible (UV-vis) experiments were completed with a UV2500 spectrophotometer (Beijing Puxi General Instrument Co., Ltd). D8 Advance polycrystalline X-ray diffractometer (XRD, Bruker AXS, Germany) was utilized to measure X-ray diffractometer spectrum. High-resolution transmission electron micrographs were supplied by a Tecnai G2 F30 S-TWIN Emission transmission electron microscope.

Synthesis of CoFe PBA. Firstly, 2 mmol of $Co(NO_3)_2 \cdot 6H_2O$ and 2.25 mmol of $C_6H_5Na_3O_7 \cdot 2H_2O$ were dissolved in 50 mL of deionized water to form solution A. Then, 1 mmol of $K_3[Fe(CN)_6]$ was dissolved in 50 mL of deionized water to form solution B. Then, solution B was added into solution A and stirred for 10 min at room temperature. After continuous stirring, the obtained mixed solution was aged for another 24 h at room temperature. The precipitate was washed via several rinsing-

centrifugation cycles with deionized water and ethanol, followed by drying at 60 °C overnight. The obtained product was designated as CoFe PBA.

Synthesis of CoFe PBA@Au brocade nanozyme. 40 mg CoFe PBA was dispersed in 10 mL of deionized water to form suspension C. 40 mg Pluronic F-127 was dissolved in 20 mL of deionized water to form solution D. Then, suspension C and solution D were mixed and stirred for 30 min at room temperature. After continuous stirring, 20 mL of $HAuCl_4$ (10 mM) was injected into the obtained mixed solution and stirred for 1 h. Then, 600 μL $NaBH_4$ (0.1 M) was added, and stirring was continued for another two hours. The obtained product was centrifuged at 10000 rpm and washed several times with deionized water.

Preparation of signal label probe (CoFe PBA@Au brocade-Ab_2). The goat anti-HIgG, regarded as secondary antibody (Ab_2), was immobilized on CoFe PBA@Au brocade to form signal label probe via the following steps. The 2 mg CoFe PBA@Au brocade was dispersed in 2 mL of PBS (0.01 M) with ultrasonic treatment for 30 min to prepare uniform suspension. Then, 200 μL MUA (10 mM), which contains one thiol and one carboxyl located at each end of carbon chain, was injected into the mixture accompanied with stirring for 2 h. Benefiting from interaction between Au nanomaterials and thiol, CoFe PBA@Au brocade can interact with thiol of MUA to form Au-S bond, accompany with effective modification of carboxyl. Taking advantage of 100 μL EDC (10 mg/mL) and 70 μL NHS (10 mg/mL) to activate carboxyl to bind amino site of Ab_2, the CoFe PBA@Au brocade-Ab_2 conjugates were obtained by adding 50 μL goat anti-HIgG (1.0 mg/mL) into the above mixture under slow stirring at 4 °C for 5 h and centrifuged at high speed of 10000 rpm at 4 °C. The resultant precipitate was redispersed in PBS and stored in refrigerator at 4 °C for the next measurement.

Construction of CL array immunosensor. The glass slides were successively treated with piranha solution and GPTMS/toluene solution at room temperature for 12 h and 24 h, respectively so as to prepare epoxy-silanized glass slides. With the help of screen printing technology, a layer of hydrophobic non-light active film containing 48 microwells with each diameter of 2 mm and edge spacing of 4 mm in 4*12 array was

printed on silanized glass slides, and the uniform microwell can be used to fix different kinds of capture antibodies and immune reaction reagents. The capture antibodies Ab_1 of 200 μg/mL rabbit anti-HIgG were mixed with 0.8 wt% chitosan in equal volume. 5 μL of the mixed solution was evenly dripped into any lines of the immunosensor array and incubated overnight at 4 ℃. After glass slides were rinsed with the buffer solution, 5 μL of BSA was dripped to block the remaining reactive sites overnight. After blocking, the prepared array immunosensors were dipped into PBS and stored at 4 ℃ before use.

CL imaging immunoassay procedure. Typically, the standard solution of HIgG was diluted with PBS (0.01 M pH 7.4) to various concentrations. Subsequently, 5 μL of HIgG with different diluted concentrations were dripped into the immunosensor to incubate with Ab_1 for 30 min. Next, the CoFe PBA@Au brocade-Ab_2 probe was dropped to the immune microwell to interact with HIgG for another 25 min, resulting in the formation of a stable sandwich immune complex. Next, 5 μL of CL substrate was added to initiate the CL reaction by CoFe PBA@Au brocade-Ab_2, and the resulting CL imaging signals were captured using a CCD camera with dynamic integration for a duration of 300 seconds. These signals were observed as spot patterns of varying intensity. Through this methodology, a stable and highly sensitive CL imaging immunoassay of HIgG was successfully conducted.

The characterizations of CoFe PBA@Au nanozyme brocade.

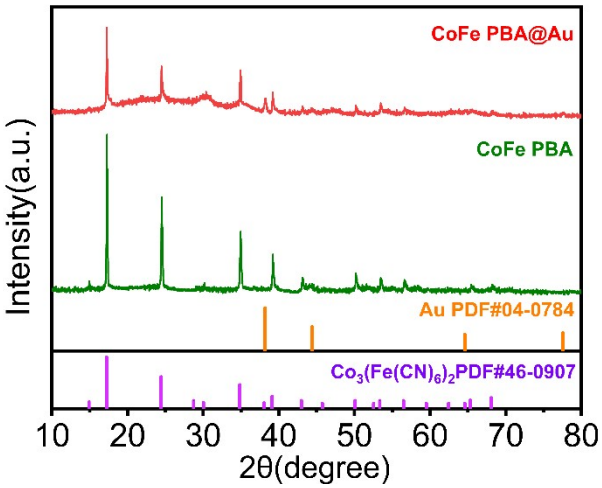

Fig. S1. XRD patterns of CoFe PBA and CoFe PBA@Au.

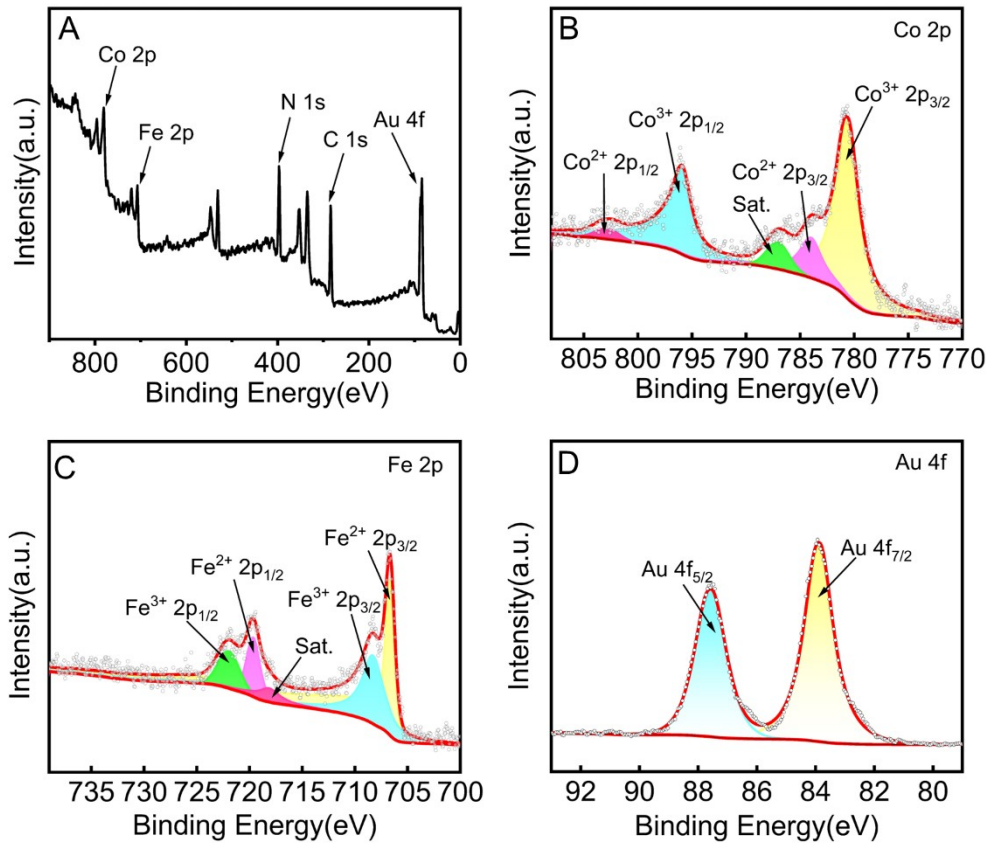

Fig. S2. XPS analysis of CoFe PBA@Au: (A) full-survey spectrum; (B) Co 2p spectrum; (C) Fe 2p spectrum; (D) Au 4f spectrum.

Reproducibility verification. The enzyme activity of CoFe PBA@Au brocade nanozyme synthesized from 5 batches was verified through UV-vis spectra, and as shown in Fig. S3, the RSD of the UV absorption intensity was 2.23%, which proved that the nanozyme was synthesized with good reproducibility.

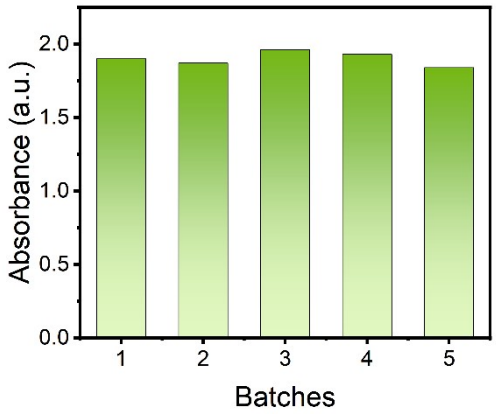

Fig. S3. Absorption peak intensity at 652 nm using UV-Vis spectroscopy of five batches of synthesized CoFe PBA@Au brocade nanozymes in the presence of TMB with H_2O_2.

Steady-state kinetic analysis of CoFe PBA. To reveal the catalytic mechanism, the Michaelis-Menten equation, as a commonly used model for enzymatic reactions, was employed for TMB oxidation. By an assumption that the concentration of the enzyme remains unchanged during catalysis, this equation approximates the original dynamics under specific reaction conditions. Then, the steady-state kinetic experiments were performed by changing concentration of the substrate (TMB or H_2O_2) in the catalytic system. The kinetic parameters were calculated by Michaelis-Menten equation:

$$V_0 = V_{max}\frac{[S]}{[S] + K_m}$$

Where V_0 and V_{max} are the initial and maximum reaction rate, respectively, [S] represents the concentration of substrate (TMB or H_2O_2), and K_m is the Michaelis constant. The kinetic parameters were also fitted by Lineweaver-Burk model:

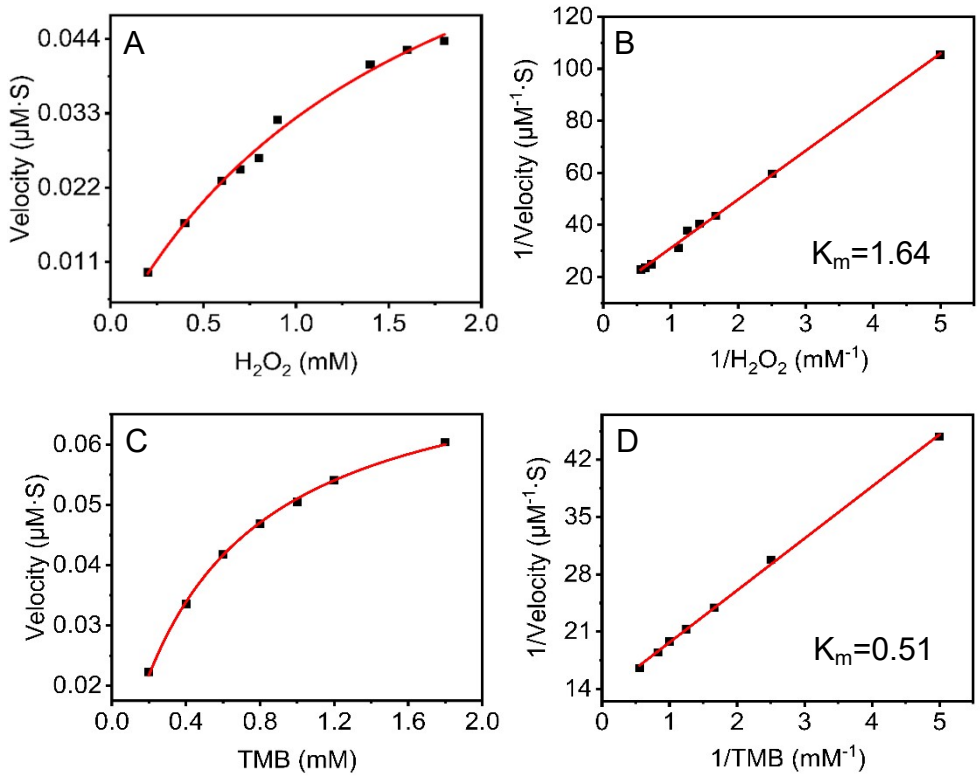

$$\frac{1}{V_0} = \frac{1}{V_{max}} + \frac{K_m}{V_{max}} \cdot \frac{1}{[S]}$$

Fig. S4. Steady-state kinetic analysis of POD-like activity of the CoFe PBA. (A, C) Kinetic analysis using Michaelis-Menten model; (B, D) Kinetic assay using Lineweaver Burk plot.

Optimization of pH for CL imaging immunoassay. pH plays an important role on activity of nanozyme. Figure S5 demonstrates the effect of different pH of the solution on the analytical performance. When the pH of the solution was increased from 5.4 to 9.4, the chemiluminescence intensity reached a maximum at pH=7.4 and then gradually decreased, which can be attributed to the fact that the antigen and the antibody have the strongest ability to bind specifically under neutral conditions.

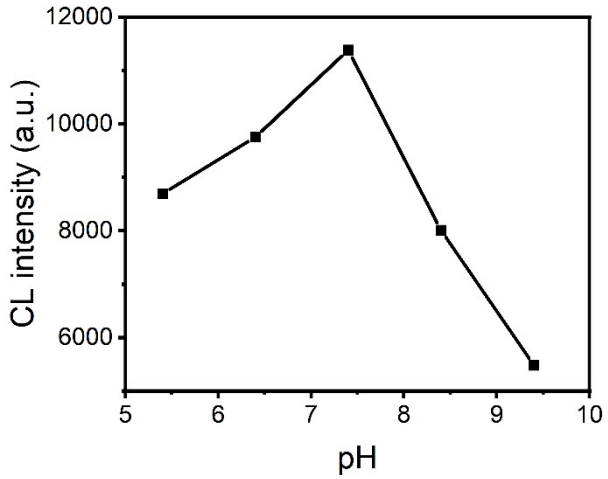

Fig. S5. pH optimization of test solution.

Optimization of incubation time. The incubation time is a critical factor in immunoassays. Hence, CL imaging intensity of the immunosensor was measured by different incubation times. This experiment includes two-step incubation. The first step can be regarded as the incubation of the Ab_1 and HIgG to form a stable immune complex. The second step is determined as immune complex incubating with CoFe PBA@Au brocade-Ab_2 probe to form sandwich immune complex. As shown in Fig. S6, when adding 10 ng/mL HIgG and CoFe PBA@Au brocade-Ab_2 probe on immunosensor, the CL imaging intensity increased correspondingly with the increase of incubation time and two step-incubation tended to be stable respectively at 30 and 25 min, respectively. Therefore, 30 min is determined as the optimal incubation time for Ab_1 and HIgG, and 25 min is determined as the optimal incubation time for HIgG and CoFe PBA@Au brocade-Ab_2.

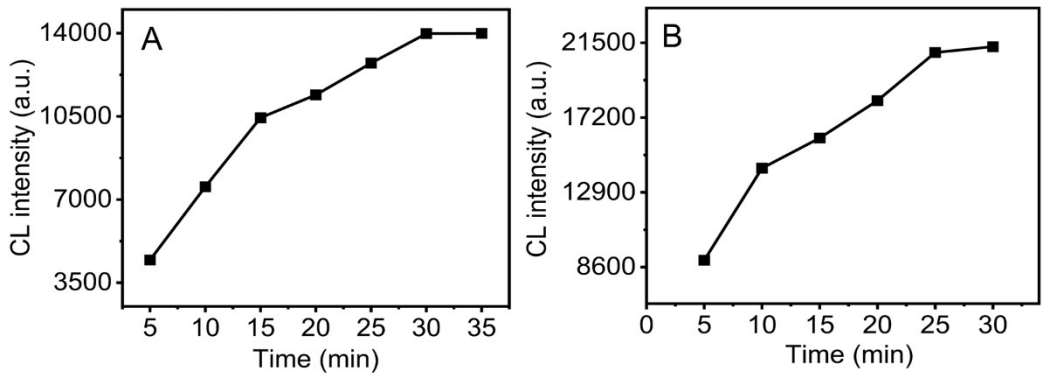

Fig. S6. Optimization of incubation time of biosensor for (A) HIgG; (B) CoFe PBA@Au-Ab_2.

Stability and reproducibility of CoFe PBA@Au brocade nanozyme-based CL imaging immunoassay. To investigate the storage stability of the established immunosensor, CL imaging signals were measured by storing the immunosensor in PBS solution at 4 °C and then recorded CL signals after saving for some days. As shown in Fig. S7A, the CL imaging intensity only reduced by 4.6% for at least 16 days. The above result shows that the immunosensor has acceptable stability. The reproducibility of the immunosensor can be evaluated by intra- and inter-variation coefficients. The variation coefficient of the intra-group can be determined by relative standard deviation of the same sample detected repeatedly five times with the same immunosensor. The variation coefficient of inter-group can be determined as relative standard deviation of the same sample detected in parallel with five different immunosensors. As shown in Fig. S7B and Fig. S7C, intra- and inter-variation coefficients of the immunosensor were 1.14% and 3.85%, indicating that the constructed CL imaging immunosensor has good reproducibility.

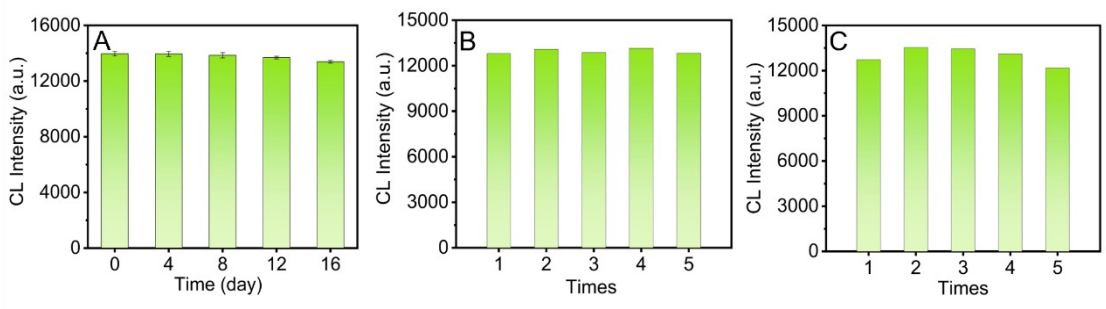

Fig. S7. (A) CL responses of the immunosensor after storage for 0 d, 4 d, 8 d, 12 d and 16 d; The intra-group (B) and inter-group (C) reproducibility of the constructed CL imaging immunosensor.

Table S1 Comparison of performance of the proposed nanozyme and other nanozymes

Catalysts	Substrate	K_m (mM)	V_{max} ($10^{-8}M \cdot S^{-1}$)	Reference
CoFe PBA@Au brocade	H_2O_2	0.69	2.3	This work
	TMB	0.30	4.0	
Zn-CuO	H_2O_2	71	0.3	S1
	TMB	10	2.877	
ZIF-67	H_2O_2	3.52	0.28	S2
	TMB	13.69	0.35	
CuO-Au nanoalloys	H_2O_2	4.08	0.0105	S3
	TMB	3.54	0.0111	
CuONRs@Au_6NPs	H_2O_2	3.11	1.27	S4
	TMB	6.34	2.44	
Graphene nanoribbons	H_2O_2	3.52	3.09	S5
	TMB	0.42	1.58	

Table S2 Comparison of performance of the proposed method and other methods

Materials	methods	Detection limit	Linear range	Reference
CoFe PBA@Au	CL	5 pg/mL	0.01-10 ng/mL	This work
Ti_3C_2-MXene/Au NPs	SPR	0.0225 μg/mL	0.075-40 μg/mL	S6
silicon/silicon dioxide	IRIS	0.25 μg/mL	1-50 μg/mL	S7
$La_{0.67}Sr_{0.33}MnO_3@SiO_2$	DPV	0.6 ng/mL	2.4-5 ng/mL	S8
poly indol-6-carboxylic acid	SWV	0.8 ng/mL	2-16 ng/mL	S9
gold-platinum nanoflower	LFI	5 pg/mL	0.05-10 ng/mL	S10

SPR: Surface plasmon resonance; IRIS: Interferometric reflectance imaging sensor; DPV: Differential pulse voltammetry; SWV: Square wave voltammetry; LFI: Lateral flow immunoassay.

Table S3 Recoveries for HIgG by the proposed CL immunosensor

Sample	Added (ng/mL)	Detected (ng/mL)	Recovery (%)
1	0.050	0.048	96.0
2	0.100	0.102	102.3
3	0.500	0.498	99.6
4	1.000	1.042	104.2
5	10.000	10.131	101.3

References

S1 A. Nagvenkar, A. Gedanken, *ACS Appl. Mater. Interfaces* 2016, **8,** 22301-22308.

S2 S. J. Wang, D. P. Xu, L. Ma, J. X. Qiu, X. Wang, Q. L. Dong, Q. Zhang, J. Pan, Q. Liu, *Anal. Bioanal. Chem.* 2018, **410,** 7145-7152.

S3 S. Mvango, P. Mashazi, *Mater. Sci. Eng. C* 2019, **96,** 814-823.

S4 S. Sicwetsha, O. Adeniyi, P. Mashazi, *RSC Adv.* 2021, **11,** 28818-28828.

S5 S. Rostami, A. Mehdinia, A. Jabbari, *Mater. Sci. Eng. C Mater. Biol. Appl.* 2020, **114,** 111034.

S6 X. Q. Zhao, Y. Zhang, X. H. Wang, P. Y. Ma, D. Q. Song, Y. Sun, *Anal. Bioanal. Chem.* 2022, **414,** 2355-2362.

S7 M. Bakhshpour, E. Chiodi, I. Celebi, Y. Saylan, N. L. Ünlü, M. S. Ünlü, A. Denizli *Biosens. Bioelectron.* 2022, **201,** 113961.

S8 A. Shore, Z. Mazzochette, A. Mugweru, *Microchim. Acta* 2016, **183,** 475-483.

S9 E. Martinez-Sade, F. Martinez-Rojas, D. Ramos, M. J. Aguirre, F. Armijo, *Polymers,* 2023, **15,** 1168-1168.

S10 J. Zhang, Q. C. Yu, W. W. Qiu, K. Li, L. S. Qian, X. J. Zhang, G. D. Liu, *Microchim. Acta* 2019, **186,** 9.